# Temtamy Preaxial Brachydactyly Syndrome Is Caused by Loss-of-Function Mutations in Chondroitin Synthase 1, a Potential Target of BMP Signaling

Yun Li,[1,2,15] Kathrin Laue,[3,15] Samia Temtamy,[4] Mona Aglan,[4] L. Damla Kotan,[5] Gökhan Yigit,[1,2] Husniye Canan,[6] Barbara Pawlik,[1,2] Gudrun Nürnberg,[1,7,8] Emma L. Wakeling,[9] Oliver W. Quarrell,[10] Ingelore Baessmann,[7] Matthew B. Lanktree,[11] Mustafa Yilmaz,[12] Robert A. Hegele,[11] Khalda Amr,[4] Klaus W. May,[13] Peter Nürnberg,[1,7,8] A. Kemal Topaloglu,[14] Matthias Hammerschmidt,[1,3,8,*] and Bernd Wollnik[1,2,8,*]

Altered Bone Morphogenetic Protein (BMP) signaling leads to multiple developmental defects, including brachydactyly and deafness. Here we identify chondroitin synthase 1 (CHSY1) as a potential mediator of BMP effects. We show that loss of human CHSY1 function causes autosomal-recessive Temtamy preaxial brachydactyly syndrome (TPBS), mainly characterized by limb malformations, short stature, and hearing loss. After mapping the *TPBS* locus to chromosome 15q26-qterm, we identified causative mutations in five consanguineous TPBS families. In zebrafish, antisense-mediated *chsy1* knockdown causes defects in multiple developmental processes, some of which are likely to also be causative in the etiology of TPBS. In the inner ears of zebrafish larvae, *chsy1* is expressed similarly to the BMP inhibitor *dan* and in a complementary fashion to *bmp2b*. Furthermore, unrestricted Bmp2b signaling or loss of Dan activity leads to reduced *chsy1* expression and, during epithelial morphogenesis, defects similar to those that occur upon Chsy1 inactivation, indicating that Bmp signaling affects inner-ear development by repressing *chsy1*. In addition, we obtained strikingly similar zebrafish phenotypes after *chsy1* overexpression, which might explain why, in humans, brachydactyly can be caused by mutations leading either to loss or to gain of BMP signaling.

## Introduction

Brachydactylies are characterized by finger and toe shortening caused by short or absent metacarpus or metatarsus and/or phalanges. They can occur either as an isolated trait or as part of a syndrome in combination with other developmental malformations. Recent analyses have identified mutations in components of the Bone Morphogenetic Protein (BMP) signaling pathway or its modulators as the cause of different types of brachydactyly. According to current concepts, loss of BMP signaling, as for example caused by loss-of-function mutations in the BMP ligand GDF5 (MIM 601146) or the GDF5 high-affinity receptor BMPR1B (MIM 603248), leads to reduced bone formation and brachydactyly type A2 (BDA2 [MIM 112600]) or type C (BDAC [MIM 113100]),[1] whereas gain of BMP signaling, as manifested by loss-of-function mutations in the BMP inhibitor Noggin (MIM 602991), can result in compromised joint formation between the different bony hand and foot elements and in the development of symphalangism (SYM1 [MIM 185800]) and/or multiple synostosis syndrome (SYNS1 [MIM 186500]).[2] However, the effects of BMP signaling seem to be more complex and subject to intensive fine tuning. For instance, in addition to being caused by loss of GDF5 activity, BDA2 can also be caused by gain of BMP2 signaling, and brachydactyly type B2 (BDB2 [MIM 611377]) can be caused by missense mutations in Noggin (Mundlos[1] and references therein). Similarly, both GDF5 and Noggin mutations are linked to deafness in SYNS1.[3] In light of this, the exact roles of BMP signaling and the nature of mediators accounting for the differential effects remain largely obscure.

The Temtamy preaxial brachydactyly syndrome (TPBS [MIM 605282]) is an autosomal-recessive congenital syndrome mainly characterized by bilateral, symmetric preaxial brachydactyly and hyperphalangism of digits, facial dysmorphism, dental anomalies, sensorineural hearing loss, delayed motor and mental development, and growth retardation.[4]

Here we mapped the *TPBS* locus to chromosome 15q26-qterm and identified causative mutations in *CHSY1* (MIM 608183) in five TPBS families. The zebrafish has recently emerged as a suitable animal model for human development and disease.[5] We show that in developing zebrafish,

[1]Center for Molecular Medicine Cologne, University of Cologne, Cologne, Germany; [2]Institute of Human Genetics, University Hospital Cologne, University of Cologne, Cologne, Germany; [3]Institute of Developmental Biology, University of Cologne, Cologne, Germany; [4]Departments of Clinical and Molecular Genetics, Division of Human Genetics and Human Genome Research, National Research Centre, Cairo, Egypt; [5]Department of Biotechnology, Institute of Sciences, Cukurova University, Adana, Turkey; [6]Department of Forensic Medicine, Faculty of Medicine, Cukurova University, Adana, Turkey; [7]Cologne Center for Genomics, University of Cologne, Cologne, Germany; [8]Cologne Excellence Cluster on Cellular Stress Responses in Aging-Associated Diseases, University of Cologne, Cologne, Germany; [9]North West Thames Regional Genetic Service, Harrow, London, UK; [10]Sheffield Clinical Genetics Service, Sheffield Children's Hospital, Sheffield, UK; [11]Blackburn Cardiovascular Genetics Laboratory, Robarts Research Institute, University of Western Ontario, London, Ontario, Canada; [12]Department of Pediatric Allergy and Immunology, Faculty of Medicine, Cukurova University, Adana, Turkey; [13]Genomatix Software GmbH, München, Germany; [14]Department of Pediatric Endocrinology, Faculty of Medicine, Cukurova University, Adana, Turkey
[15]These authors contributed equally to this work
*Correspondence: mhammers@uni-koeln.de (M.H.), bwollnik@uni-koeln.de (B.W.)
DOI 10.1016/j.ajhg.2010.10.003. 

loss and gain of *chsy1* function lead to defects similar to those in human TPBS patients. Such defects include reduced body length, compromised formation of the pectoral fin, severe midline deficiencies in the cartilage of the neurocranium, and compromised formation of epithelial protrusions and semicircular canals in the inner ear. Moreover, we demonstrate that Bmp signaling has a negative effect on *chsy1* expression and that Dan is required for inhibition of Bmp signaling and derepression of *chsy1* expression in epithelial protrusions, and it thereby allows semicircular canal morphogenesis.

## Material and Methods

### Subjects

All subjects or their legal representatives gave written informed consent to the study. The study was performed in accordance to the Declaration of Helsinki protocols and approved by the local institutional review boards. Five families with the clinical diagnosis of Temtamy preaxial brachydactyly (TPBS) were included in the study. Clinical features of some of the families have been already published: TPB1,[4] TPB4,[6] and TPB5.[7] Patients underwent general otological examinations and pure-tone audiometry with air and bone conduction at 250 Hz, 500 Hz, 1000 Hz, 2000 Hz, 4000 Hz, and 8000 Hz. Vestibular evaluation in affected individuals did not reveal any symptoms of vestibular dysfunction. Moderate to profound sensorineural hearing impairment was diagnosed in families TPB1 (individual II-2), TPB2 (individual II-2), TPB3 (individuals II-3 and II-5), TPB4 (individual II-2), and TPB5 (individuals II-5 and II-6). DNA from participating family members was extracted from peripheral blood lymphocytes by standard extraction procedures.

### Linkage Analysis

Genome-wide linkage analysis in available members of the TB1 and TB2 families was performed with the Affymetrix GeneChip Human Mapping 10K SNP Array Xba142 (version 2.0). Genotypes were called by the GeneChip DNA Analysis Software (GDAS v3.0, Affymetrix). We verified sample genders by counting heterozygous SNPs on the X chromosome. Relationship errors were evaluated with the help of the program Graphical Relationship Representation.[8] The program PedCheck detected Mendelian errors,[9] and data for SNPs with such errors were removed from the data set. Non-Mendelian errors were identified with the program MERLIN,[10] and unlikely genotypes for related samples were deleted. Linkage analysis was performed under the assumption of autosomal-recessive inheritance, full penetrance, consanguinity, and a disease gene frequency of 0.0001. Multipoint LOD scores were calculated with the program ALLEGRO.[11] Haplotypes were reconstructed with ALLEGRO and presented graphically with HaploPainter.[12] All data handling was performed with the graphical user interface ALOHOMORA.[13] For the TPB3 family, an independent genome-wide 250K NspI Affymetrix SNP Array (Affymetrix, CA, USA) analysis was done on all members of the nuclear family at the Genome Sciences Laboratory of the Ankara University Biotechnology Institute. SNP Array data were analyzed by Genespring GT (Agilent, Santa Clara, CA, USA). For subsequent fine mapping, known and newly designed microsatellite markers for the critical region were genotyped (Table S2).

### Mutation Screening

We searched databases to identify candidate genes in the critical region on chromosome 15q26-qterm (GeneDistiller, Ensemble Genome Server, and UCSC Genome Bioinformatics). Four candidate genes, *ADAMTS17* (MIM 607511), *CHSY1*, *SELS* (MIM 607918), and *PCSK6* (MIM 167405), were chosen for mutation screening on the basis of their expression pattern and presumed functional properties (OMIM and Unigene). Primers were designed according to the reference sequences. The coding exons and adjacent splice sites of these candidate genes were sequenced in the index patients of TPB1 and TPB2 families. We amplified the three exons of *CHSY1* (*CHSY1*, NC_000015.9; CHSY1, NP_055733.2; Table S2) from DNA of all affected members of the five families and sequenced the PCR products by BigDye Terminator method on an ABI 3100 sequencer. We resequenced all identified mutations in independent experiments and tested for cosegregation within the families. We tested 150 healthy control individuals from Turkey, 30 from Morocco, and 30 from Egypt for the mutations in exon 1 (c.55-84del30, c.14delG, and c.205C>T) by direct sequencing. One hundred twenty controls from Pakistan and 40 from Turkey were tested for the mutation of c.321−3C>G by PCR and restriction digestion, and 150 controls from Pakistan were tested for the p.P539R mutation. CHSY protein sequence was analyzed with the server Pfam for protein domains. All primer sequences of designed polymorphic markers on 15qter and primer sequences for genomic and cDNA amplification of *CHSY1* can be found in Table S2.

### *CHSY1* cDNA Analysis

RNA was extracted from fresh blood with the Paxgene Blood RNA system (QIAGEN). Reverse-transcriptase polymerase chain reaction (RT-PCR) was performed with RevertAid First Strand cDNA synthesis Kit (Fermentas). The primers for amplification were designed according to the reference sequence and located in exon 1 and exon 3 (*CHSY1* mRNA, NM_014918.4; Table S2).

### Histology

Whole-mount in situ hybridizations, immunostainings, and double in situ hybridizations were carried out as described.[14,15] For *chsy1* probe synthesis, a 1030 bp fragment of zebrafish *chsy1* cDNA (GenBank accession number BC064670[16]) was amplified via RT-PCR, cloned into pCRII (Invitrogene), linearized with HindIII, and transcribed with T7 RNA polymerase. Sense control probe was generated with NotI and SP6 RNA polymerase. The *bmp2b*, *msxc*, and *sox9a* probes were generated as described.[17–19] Fluorescein-phalloidin staining of hair cells in sensory patches of inner ears was carried out as described.[17]

### Morpholino Injection

Two sequence-independent antisense morpholino oligonucleotides (MOs) targeting the translational start codon (*chsy1*-ATG MO) or 5′ untranslated region (*chsy1*-UTR MO) were purchased from GeneTools. Sequences were as follows: *chsy1*-ATG MO, 5′-AAGATCTGCGACTCCTTCCTGCCAT-3′ (identical to MO in Zhang et al.[16] and Peal et al.[20]); and *chsy1*-UTR MO, 5′-CTAG TCGCTTTAATTTGTCAGAGTT-3′. MOs were injected into 1- to 4-cell-stage embryos, as described;[21] per embryo, 1.5 nl was injected at concentrations ranging from 66–333 μM (ATG MO) and from 333–500 μM (UTR MO). To avoid unspecific toxicity, we coinjected the UTR MO with p53-MO.[22] To control knockdown efficacy, we cloned the 5′ UTR and the first 46 nucleotides

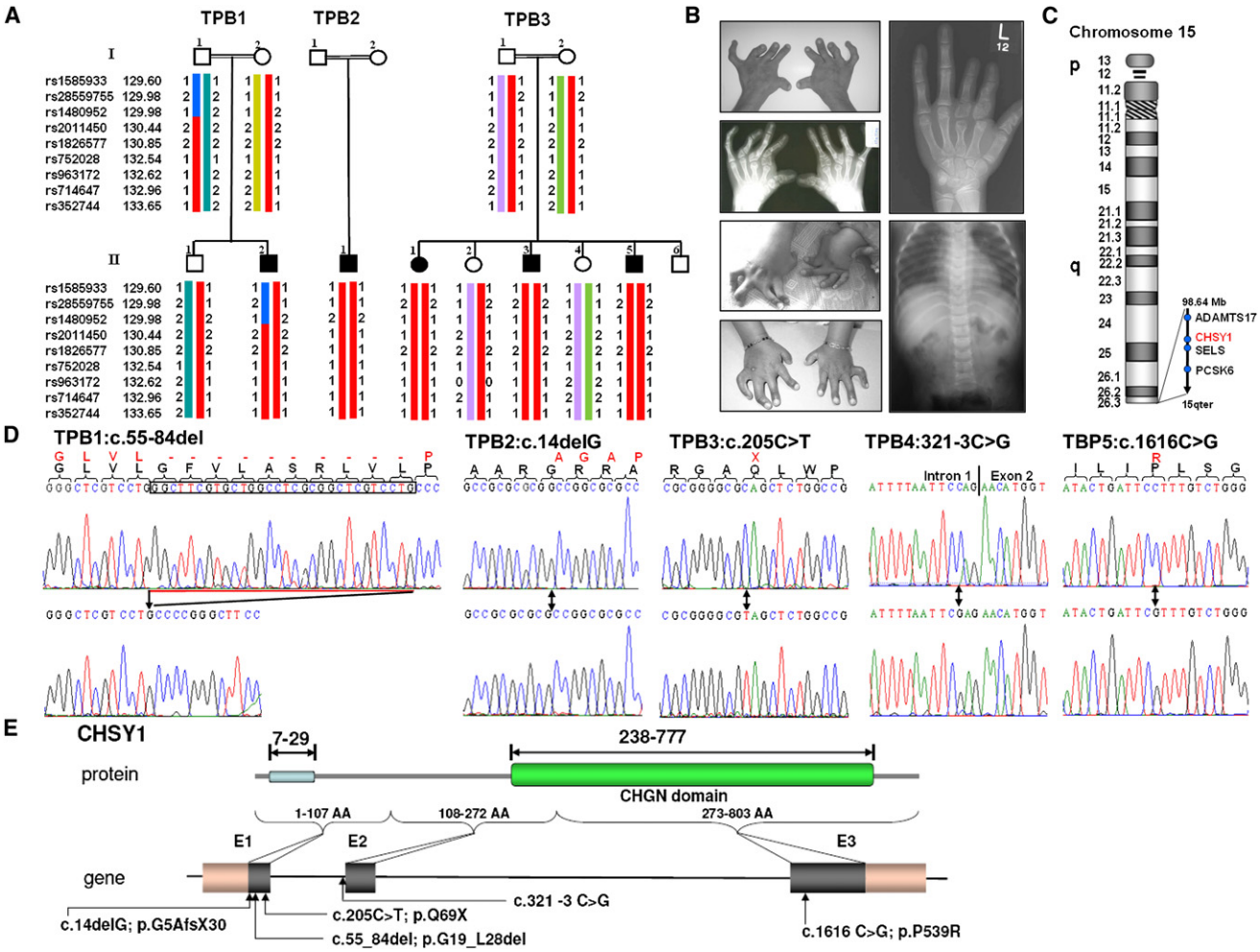


**Figure 1. Clinical and Molecular Findings in Families with TPBS**
(A) A haplotype analysis of the 15q26-qterm critical region indicates homozygosity in affected individuals of the TPB1, TPB2, and TPB3 families.
(B) Typical hand anomalies and skeletal findings seen in our patients with TPBS.
(C) Genomic overview of the 15q26 critical region and genomic localization of the genes tested.
(D) Electropherograms of identified homozygous *CHSY1* mutations compared to wild-type sequences. Above, wild-type sequences are shown.
(E) Schematic view of CHSY1 protein domains, coding exons, and localization of identified *CHSY1* mutations.

of the coding region into pCS2+ vector[23] and fused it to GFP. The plasmid was linearized with NotI, and *chsy1-gfp* hybrid mRNA was generated with the SP6 MessageMachine Kit (Ambion, Austin, TX). Injection of this mRNA into zebrafish embryos yielded strong GFP fluorescence at late gastrula stages (Figure S3). However, fluorescence was completely suppressed upon subsequent coinjection of the mRNA with *chsy1*-ATG MO or *chsy1*-UTR MO (Figure S3). *dan* MO injections were done as described.[24]

### Overexpression Studies

For *chsy1* overexpression, the coding region of human *CHSY1* was cloned into the Cla1 and XhoI sites of pCS2+.[23] The plasmid was linearized with NotI, and capped sense RNA was synthesized in vitro via the SP6 MessageMachine Kit (Ambion, Austin, TX). mRNA (1.5 nl) was injected into 1- to 4-cell-stage embryos at a concentration of 100 ng/μl. For temporally controlled *bmp2b* overexpression, the offspring of *Tg(hsp70l:bmp2b)fr13* transgenic fish were subjected to a 30 min heat shock (transfer from 28°C to 39°C) at 48 hpf, as described.[25]

## Results

### Clinical Findings in TPBS Families

We have examined five TPBS families presenting with a variable expression of clinical symptoms (Figure 1A, B, and Table 1). We observed mild facial dysmorphism, including round face and craniosynostosis, mild hypertelorism, and micrognathia, in the majority of TPBS cases (Table 1). Distal limb anomalies affected both hands and feet and were characterized by short and abducted thumbs, short and deviated halluces, and syndactyly. Typical preaxial brachydactyly of digits 1–3 was seen in all affected individuals and, in addition, hyper- and symphalangism, radio-ulnar synostosis, and carpal or tarsal fusions were observed in X-rays of

**Table 1. Clinical Findings in TPBS Families Carrying *CHSY1* Mutations**

| Family Data | TB-1 | TB-2 | TB-3 | TB-4 | TB-5 |
|---|---|---|---|---|---|
| Consanguinity | + | + | + | + | + |
| Number of affected individuals | 1 | 2 | 3 | 1 | 3 |
| Mutation (nucleotide change) | c.55-84del | c.14delG | c.205C>T | c.321−3C>G | c.1616C>G |
| Mutation (protein change) | G19_L28del | G5AfsX30 | Q69X | – | P539R |
| Origin | Egypt | Egypt | Turkey | Sri Lanka | Pakistan |
| **Facial Dysmorphism** | | | | | |
| Plagiocephaly | + | + | +/– | – | – |
| Hypertelorism | + | + | – | + | – |
| Micro- or retrognathia | + | + | – | – | – |
| **Dental Anomalies** | | | | | |
| Microdontia | + | + | + | + | + |
| Talon cusps | + | + | + | + | – |
| **Hearing Loss** | | | | | |
| Sensorineural | + | + | + | + | + |
| Conductive | – | – | – | – | + |
| Malformed ears | + | + | + | ? | – |
| **Hand or Foot Anomalies** | | | | | |
| Short fingers or toes I, II, III | + | + | + | + | + |
| Syndactyly | + | + | + | + | + |
| Abducted thumbs | + | + | + | + | + |
| Lateral/medial deviations of fingers/toes | + | + | + | + | + |
| Clinodactyly | + | + | + | + | + |
| **Radiological Findings** | | | | | |
| Preaxial brachydactyly | + | + | + | + | + |
| Short metacarpals/metatarsals | + | + | + | + | + |
| Hyperphalangism | + | + | + | + | + |
| Symphalangism | + | + | + | + | + |
| Phalangeal duplications | + | + | + | + | + |
| Radioulnar synostosis | – | – | – | + | – |
| **Skeletal Anomalies** | | | | | |
| Kyphoscoliosis | + | + | +/– | – | – |
| Pectus excavatum | + | – | – | – | – |
| Generalized osteoporosis | + | + | + | n.a. | n.a. |
| **Additional Findings** | | | | | |
| Developmental delay | + | + | + | ? | – |
| Mental retardation | + | + | + | ? | – |
| MRI findings | n.a. | partial agenesis of the cerebellar vermis | cerebellar degeneration, mild brain stem atrophy | n.a. | n.a. |
| Optic atrophy | – | – | – | + | – |

some cases. Further skeletal anomalies showed a progressive course in TPBS patients and included growth retardation, kyphoscoliosis, and pectus excavatum. Interestingly, we found moderate to profound sensorineural hearing loss in almost 80% of the cases.

### Mapping of the TPBS Locus and Identification of CHSY1 Mutations

Initially, we genotyped DNA samples from available family members of the originally described TPB1 family (4) and one additional family, TPB2, which both originated from Egypt, by using the Affymetrix GeneChip Human Mapping 10K SNP Array (version 2.0). Affected individuals were born to consanguineous parents in both families. Two possibly linked loci on chromosomes 1p33 and 15q26 were observed and had a combined parametric LOD score of 2.37 and 2.51, respectively (Figure S1). Extensive analysis of microsatellite markers of these regions mapped the *TPBS* locus to chromosome 15q26-qterm between SNPs rs1480952 and rs352744 (Figure 1A; see also Figure S2), defining a shared homozygous critical interval of approximately 3.8 Mb and excluding the 1p33 region (Figure 1C; see also Figure S2). Mapping data of one additional TPBS family, TPB3 from Turkey, confirmed the *TPBS* locus without reducing the critical region (Figure 1A).

Among the 20 annotated genes within this region, we sequenced four of them as highly relevant positional candidate genes (*ADAMTS17*, *CHSY1*, *PCSK6*, and *SELS*; Table S1). Sequencing of the three coding exons of the chondroitin synthase 1, *CHSY1*, gene revealed different homozygous mutations in affected individuals in each of the three linked families as well as two additional families with TPBS, which were subsequently tested. *CHSY1* is transcribed to a 4549 bp transcript (NM_014918.4), which encodes a protein of 803 amino acids. All mutations cosegregated with the disease in the families and were not found in more than 150 healthy control individuals. We found three mutations in exon 1 of *CHSY1*: a 30 bp deletion, c.55-84del (p.G19_L28 del, TPB1 family); a 1 bp deletion, c.14delG (p.G5A*fs*X30, TPB2 family); and the c.205C>T nonsense mutation (p.Q69X) in all three affected individuals of the TPB3 family (Figures 1D and 1E). An acceptor splice-site mutation, c.321-3C>G, was identified in the TPB4 family, whereas the only missense mutation, c.1616C>G (p.P539R, TPB5 family), was located in exon 3 of the gene (Figures 1D and 1E).

The acceptor splice-site mutation c.321−3C>G is predicted to cause skipping of *CHSY1* exon 2 and lead to the loss of 496 bp on the transcript level and thus a frame shift and premature protein truncation. We confirmed skipping of exon 2 on cDNA of the affected individual (Figures S2A and S2B). The only missense mutation identified, p.P539R, affects a highly conserved proline (Figure 2C).

### Expression of *chsy1* in Zebrafish

No *Chsy1* knockout mice have been reported yet. However, consistent with the phenotypic traits of TPBS, our in situ hybridization analysis revealed *Chsy1* expression in chondrocytes and the developing inner ear of E12.5 and E14.5 mouse embryos (data not shown). To address the developmental functions of CHSY1 and CS, and their possible relationship to BMP signaling, we turned to the zebrafish system. Whole-mount in situ hybridization revealed widespread expression of *chsy1* in the head (data not shown) and prominent expression in the floor plate (Figure 3A) and the fin epithelium (Figures 3B and 3D) of wild-type zebrafish embryos at 24 hr postfertilization (hpf). During the second day of development, prominent expression was also detected in the heart (data not shown), chondrocytes of the developing head skeleton (Figure 3E), pharyngeal endoderm of the branchial arches (Figure 3F,G), distal regions of the pectoral fin buds (Figure 3H), and epithelial protrusions of the inner ears (Figure 3I). These protrusions later fuse to form the semicircular canal ducts; the central components of the vestibular system contribute to angular motion sensing and body balancing.[26] After this fusion has occurred, *chsy1* transcript levels appear to drop (Figure 3J).

### Phenotypes of Zebrafish after Loss and Gain of *chsy1* Activity and the Correlation of *chsy1* to *bmp2b* and *dan*

To knock down Chsy1 activity, we injected zebrafish embryos with antisense morpholino oligonucleotides (MOs; for efficacy control; see Figure S3). In addition, for gain-of-function studies, we injected in vitro synthesized human *CHSY1* mRNA. Surprisingly, both treatments led to similar defects, including a significant reduction of body length (Figures 4A–4C), compromised pectoral fin formation (Figures 4D–4F), severe midline deficiencies in the cartilage of the neurocranium (Figures 4G and 4H), notochord undulation (Figures 4K and 4L), and later, notochord degeneration (Figures 4I and 4J), which could be correlated with the aforementioned *chsy1* expression in the overlying floorplate cells (see above; Figure 3A) and with the shorter body length (Figure 4B). Furthermore, *chsy1* morphants displayed reduced eye distances, as well as slight cyclopia in severe cases (Figures 4M–4O), which is linked with the neurocranial deficiencies (Figures 4G and 4H). In addition, the eyes developed colobomas (Figures 4P–4R).

In the inner ears, formation of epithelial protrusions and semicircular canals was severely compromised (Figures 5A–5D). However, according to *msxc* in situ hybridization and FITC-phalloidin staining of hair cells, the cristae and maculae, semicircular canal- and otolith-associated sensory patches of the ear, respectively, did not show major alterations in *chsy1* morphants (Figures 5K–5N). This suggests that, rather than being important for hair cell development itself, Chsy1 might be instrumental for proper morphogenesis of the vestibular organ.

Positive and negative effects on semicircular canal development have also been reported for BMP signaling. Although according to genetic analysis, late loss of Bmp2b function leads to defective semicircular canal morphogenesis,[27] another report describes similar effects

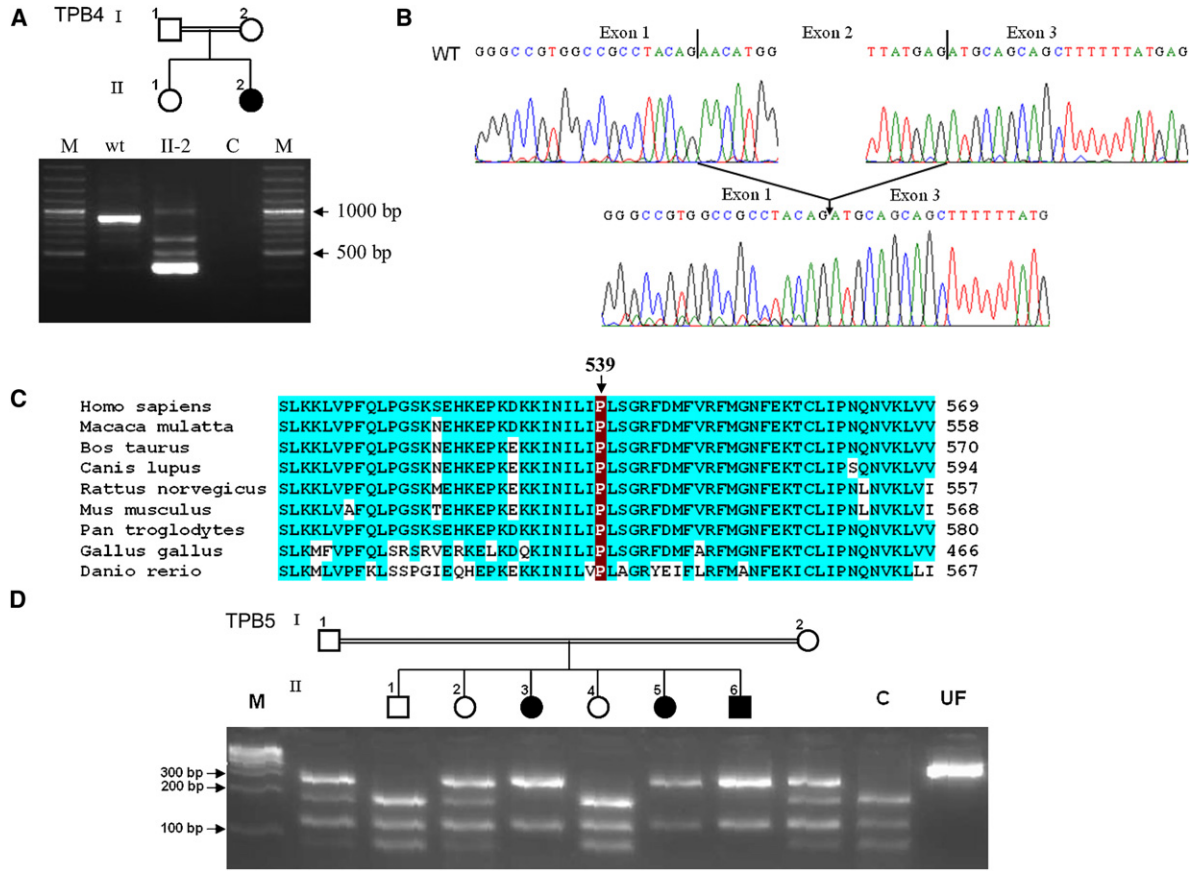


**Figure 2. Additional Molecular Findings in TPBS**

(A) Amplification of *CHSY1* cDNAs of the TPB4 patient carrying the c.321−3C>G splice-site mutation and of a healthy control. The forward primer was located in exon 1, and the reverse primer was located in exon 3. Complete loss of the normal amplicon size in the patient's cDNA was due to the skipping of exon 2. Abbreviations are as follows: M, marker; WT, wild-type control; and C, water control without DNA.

(B) Electropherograms of *CHSY1* transcripts from the wild-type control and patient TPB4 show the skipping of exon 2 in the patient.

(C) An amino acid sequence alignment of CHSY1 proteins of different species shows the highly conserved proline at position 539.

(D) A PCR and enzyme-digestion method was used as a second independent method of showing the cosegregation of the c.1616C>G (p.P539R) missense mutation in the TPB5 family. The mutation abolishes one of the two *Bsl I* restriction sites in the amplicon. Parents were heterozygotes, and all three patients (II3, II5 and II6) were homozygotes for the mutation, whereas none of the three healthy siblings had the homozygous mutation. Abbreviations are as follows: M, Marker; C, healthy control individual; and UF, undigested PCR fragment.

under Bmp2b/4 gain-of-function conditions.[28] *bmp2b* and *chsy1* are expressed in a largely complementary manner. At 56 hpf, *bmp2b* expression is strongest in the developing cristae of the inner ear (Figure 5J), where *chsy1* expression is very weak (Figure 5G). In contrast, the epithelial protrusions display strong expression of *chsy1* (Figure 5G) and the Bmp inhibitor *dan*[24] but weak *bmp2b* expression (Figure 5J). Consistently, transgenic overexpression of *bmp2b* during the second day of development or MO-mediated knockdown of *dan* led to impaired semicircular-canal formation similar to that caused by knockdown of *chsy1* (Figures 5E and 5F). Furthermore, both treatments compromised *chsy1* expression in the epithelial protrusions (Figures 5H and 5I). Together, this suggests that Bmp signaling has a negative effect on *chsy1* expression and that Dan is required for inhibition of Bmp signaling and derepression of *chsy1* expression in epithelial protrusions; Dan thereby allows semicircular canal morphogenesis. It is tempting to speculate that Bmp inhibition and Chsy1 play a similar role during morphogenesis of the cochlea, the central auditory structure in mammals, and that they possibly underlie the hearing loss in human TPBS patients.

## Discussion

In the present study we showed that congenital bilateral, symmetric preaxial brachydactyly and hyperphalangism of digits, facial dysmorphism, dental anomalies, sensorineural hearing loss, and growth retardation in the Temtamy preaxial brachydactyly syndrome (TPBS) are caused by recessive mutations in *CHSY1*. The encoded protein, chondroitin synthase 1, is a key protein in the biosynthesis of chondroitin sulfate (CS). It belongs to the glycosaminoglycans (GAGs) and is composed of alternating glucuronic

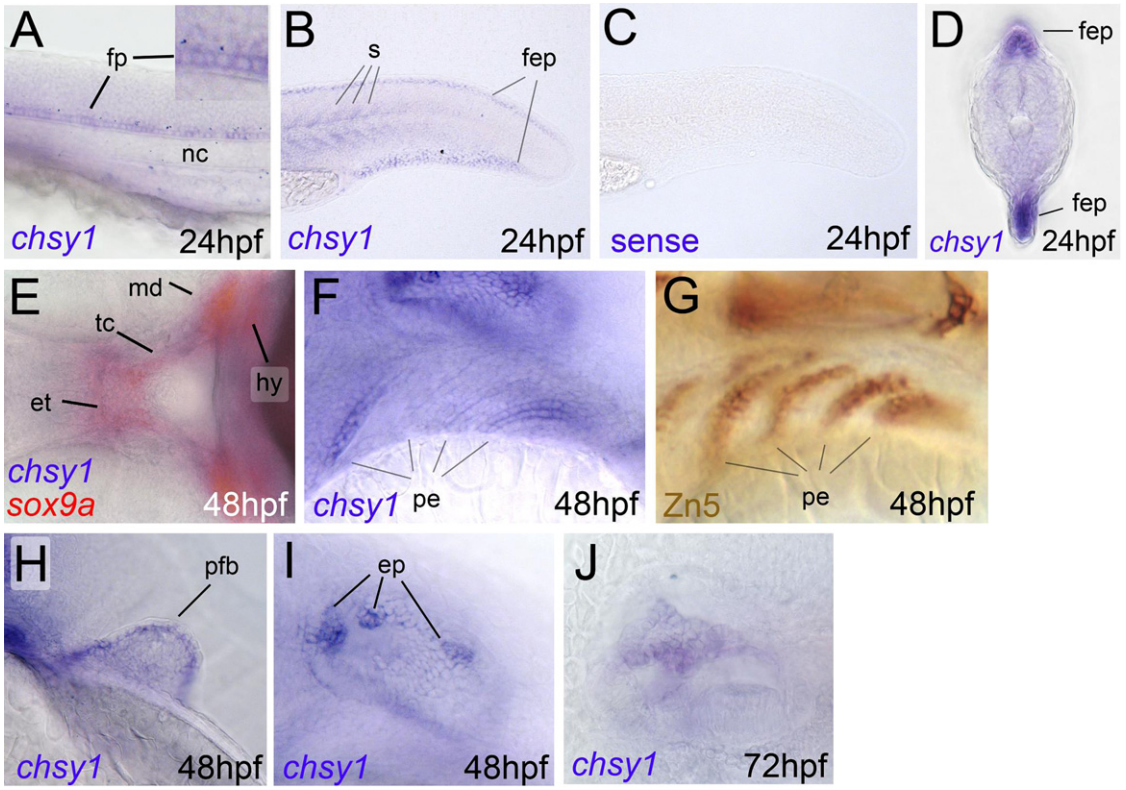


**Figure 3. Expression of *chsy1* during Zebrafish Development**

Ages of embryos and larvae (in hpf) are indicated in the lower right corners, and the in situ hybridization probes (A–F and H–J) or antibody (G) are indicated in the lower left corners. (A–C, F–J) Lateral views. Anterior is to the left. (D) A transverse section through the tail. Dorsal is to the top. (E) A ventral view of the head region.

(A–F and H–J) Whole-mount in situ hybridization with a *chsy1* antisense probe to detect *chsy1*mRNA (A, B, D, E, F, H, I, and J), *sox9a* antisense probe[19] to colabel chondrocytes (E, in red), and a *chsy1* sense control probe (C). (G) Whole-mount anti-Zn5 immunostaining, marking the pharyngeal endoderm (compare with Piotrowski and Nüsslein-Volhard [40]). *chsy1* is expressed in the floor plate (fp), located between the spinal cord and the notochord (nc) (A), in the basal keratinocyte layer of the fin epithelium (B and D), in somatic cells close to the myosepta (B), in chondrocytes of the neurocranium and pharyngeal arches of the visceral skeleton (E), in the pharyngeal endoderm (pe) of the branchial arches (F), and in epithelial protrusions of forming semicircular canals in the inner ear (I). When these epithelial protrusions have fused in the center of the otic vesicle, *chsy1* transcript levels drop (J).

Abbreviations are as follows: ep, epithelial protrusions; et, ethmoid plate (neurocranium); fep, fin epithelium; fp, floor plate; hy, hyoid (second pharyngeal arch); md, mandibular (first pharyngeal arch); nc, notochord; pe, pharyngeal endoderm; pfb, pectoral fin bud; s, somite; and tc, trabeluca cranii (neurocranium).

acid (GlcUA) and N-acetyl galactosamine (GalNAc) residues.[29] CS can be synthesized in multistep processes as covalently bound side chains of proteins known as proteoglycans.[30] CHSY1 has both the glucuronyltransferase II and N-acetylgalactosaminyl-transferase II activities required for the synthesis of the repeating disaccharide unit of CS. Both deletions and the p.Q69X nonsense mutation, all located in exon 1 of *CHSY1*, can be expected to cause structural alterations and disruption of the CHSY1 protein structure. We also confirmed that the acceptor splice-site mutation c.321−3C>G causes skipping of *CHSY1* exon 2 and leads to the loss of 496 bp on the transcript level and a frame shift and premature protein truncation. Therefore, it is likely that the c.321−3C>G mutation also leads to a nonfunctional CHSY1 protein. We only identified one missense mutation, p.P539R, which affects a highly conserved proline within the functionally important chondroitin N-acetylgalactosaminyl-transferase (CHGN) domain of CHSY1 (Figure 1E). The substitution of proline by arginine might interfere with the normal folding of this domain and thus prevent efficient protein function. Taken together, these findings demonstrate that complete or nearby complete loss of CHSY1 function underlies autosomal-recessive TPBS.

Our zebrafish study demonstrated that both loss and gain of Chsy1 function lead to similar defects during various morphogenetic processes in the zebrafish; some of these processes might be equivalent to the distal limb malformations, craniofacial dysmorphism, shorter stature, and hearing loss caused by the homozygous loss of human CHSY1 function in TPBS. The similarity of the zebrafish inner-ear phenotype after loss and gain of Chsy1 or Bmp activity, together with the loss of *chsy1* transcription after gain of Bmp signaling, further suggests that a similar deregulation of CHSY1 might at least partly underlie the different defects caused by aberrant BMP signaling in mammals. Such defects include craniofacial and inner-ear dysmorphologies[31–33] and the different types of

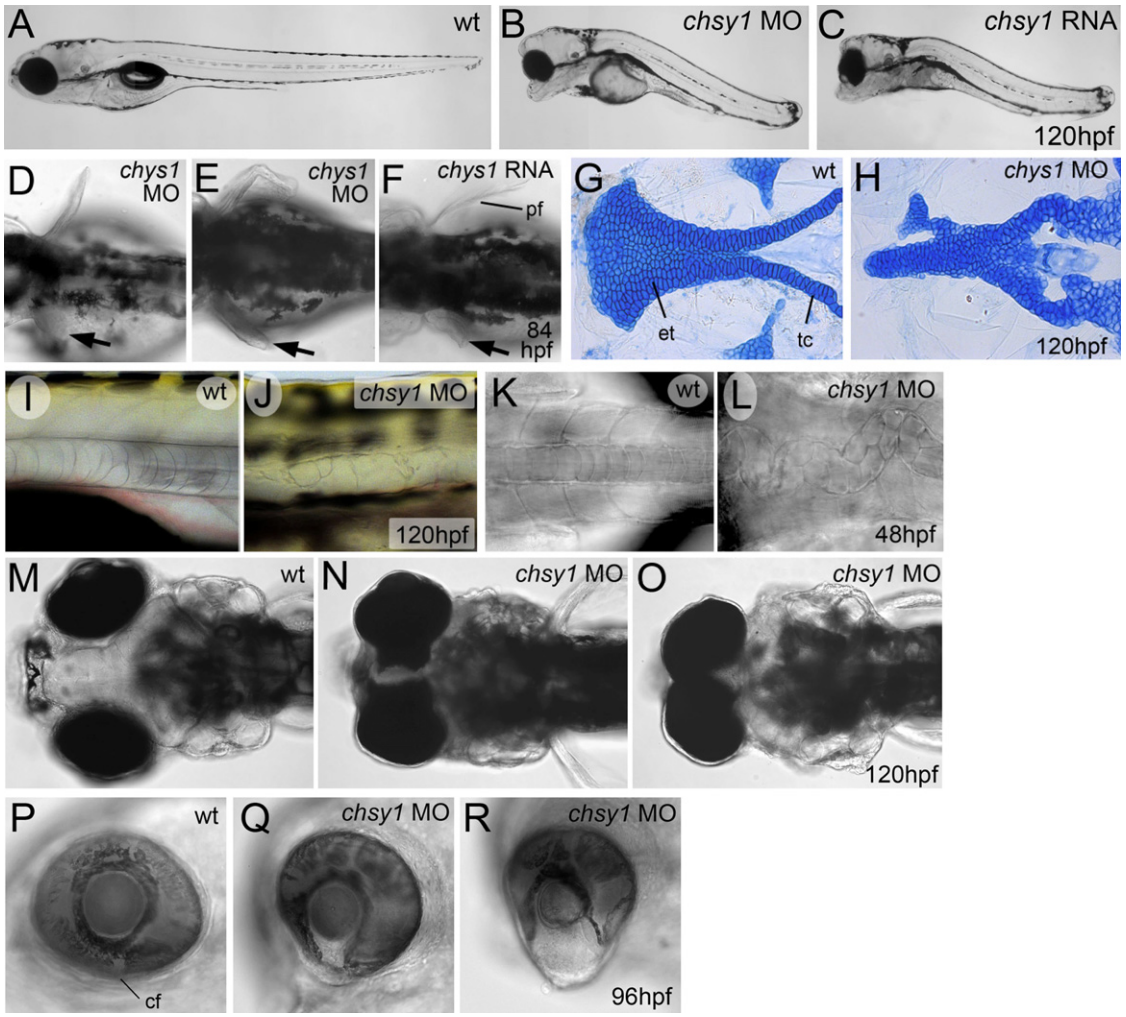


**Figure 4. Phenotypes of Zebrafish Larvae after Loss and Gain of *chsy1* Function**

Ages of zebrafish larvae (in hpf) are indicated in the lower right corners, and treatments are indicated in the upper right corners. Abbreviations are as follows: MO, embryo injected with antisense morpholino, loss of function; RNA, embryo injected with synthetic mRNA, gain of function; and wt, unjected wild-type control.

(A–C) Lateral views of live animals, displaying reduced body length and altered head morphology after *chsy1* loss and gain of function.

(D–F) Dorsal views of the anterior trunk of live larvae, displaying pectoral fins with variably reduced outgrowth. Upper fin in (F) is of normal size and shape. Compared to the other phenotypic traits, impaired fin development was only moderately penetrant (approximately 30%), and it often occurred in a unilateral manner (as in F). (G and H) Alcian blue staining of cartilage of the neurocranium. For a better appreciation of the neurocranial deficiencies, the visceral skeleton was manually removed.

(I and J) Lateral view of the trunk of live animals, revealing degeneration of notochord cells in the morphant. In several zebrafish mutants, notochord degeneration is linked to and most likely causative of reduced body length,[41] as also seen in the *chsy1* morphants described here.

(K and L) View of the trunk of live embryo. The notochord undulation of the morphant indicates that the shortened body length cannot be solely caused by notochord degeneration. Similar notochord undulation has been observed in several zebrafish mutants, e.g., those carrying loss-of-function mutations in *wnt5a*,[36] pointing to a possible additional role of Chsy1 in modulating noncanonical Wnt signaling.

(M–O) Dorsal view of the heads of live larvae. Medial expansion of the eyes and loss of midline forebrain tissue leads to partial cyclopia. Note that in the morphants shown here, the pectoral fins are not or only moderately affected.

(P–R) Lateral view of the eyes, revealing lack of dorsal retinal tissue and failed closure of the choroid fissure (coloboma). This phenotypic trait is linked to the above-described medial-forebrain deficiencies and shifts of the eyes to more medial positions, and it might be a secondary consequence of the overall alterations in head and head-skeleton morphology.

Abbreviations are as follows: cf, choroid fissure of eye; et, ethmoid plate (neurocranium); pf, pectoral fin bud; and tc, trabeluca cranii (neurocranium).

human brachydactylies, caused by either gain or loss of BMP signaling.[1] Future studies will have to reveal the molecular mechanisms of *chsy1* repression by Bmp signaling and of Chsy1 and CS function. Computational analysis of human *CHSY1* revealed the presence of several Smad transcription-factor binding sites (data not shown), suggesting that the effect of BMP signaling on *CHSY1* expression might be direct. CS, in turn, could have

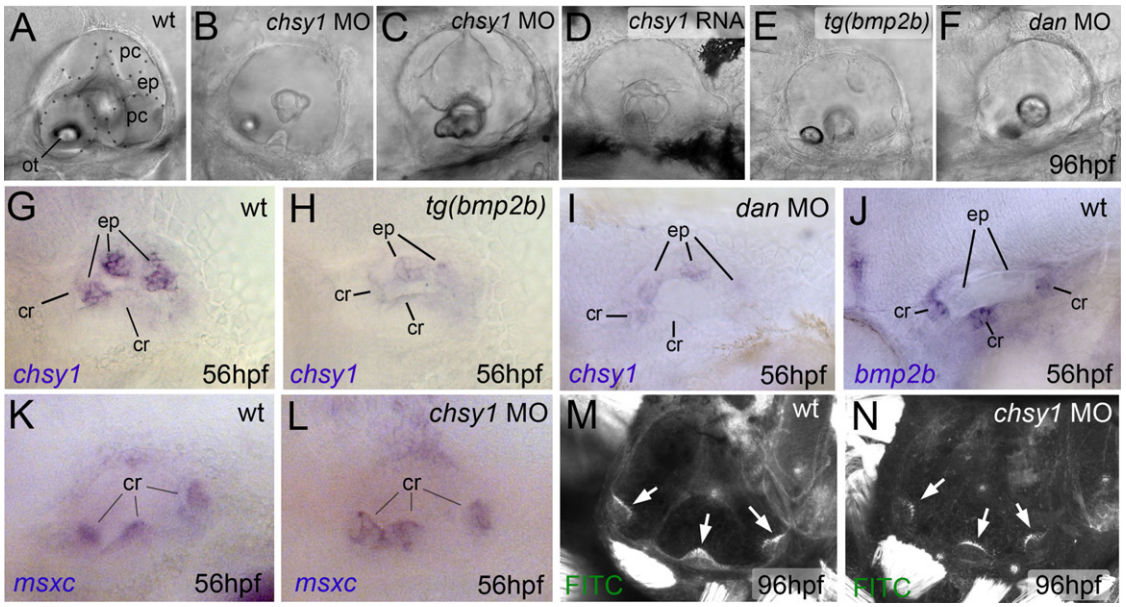


**Figure 5. Interaction between *chsy1*, *bmp2b*, and *dan* during Inner-Ear Morphogenesis**

Ages of larvae (in hpf) are indicated in lower right corners, and treatments are indicated in upper right corners. Abbreviations are as follows: MO, embryo injected with antisense morpholino; RNA, embryo injected with synthetic mRNA; tg(bmp2b), transgenic after heatshock induction of ubiquitous *bmp2b* expression;[25] and wt, unjected or nontransgenic wild-type control.

(A–F) Lateral views of the inner ear of live animals. In the wild-type control (A), the walls of the semicircular canals are outlined by dots.

(G–H) Inner ears after whole-mount in situ hybridization for *chsy1* (t-v) or *bmp2b* (w) mRNA. For details, see text.

(G–L) Lateral views of the inner ears after whole-mount in situ hybridization for *chsy1* (G–I), *bmp2b* (J), or *msxc* (K and L). (G–I) *chsy1* mRNA levels in epithelial protrusions (ep) are strongly reduced after overexpression of *bmp2b* (H) and after inactivation of the BMP inhibitor Dan (I). The much weaker expression in the cristae primordia (cr) remains unaltered (compare G and H). (J) In contrast to *chsy1* (see G), *bmp2b* is strongly expressed in the cristae of the wild-type inner ear (K and L). *msxc* expression in cristae of the *chsy1* morphant is unaltered (L). Because *msx* genes are known transcriptional targets of BMP signaling, these data also suggest that, in contrast to the BMPs upstream of *chsy1*, Chsy1 does not act upstream of BMP signaling.

(M and N) Merged stacks of confocal images of inner ears after fluorescein (FITC)-phalloidin staining. Cristae (indicated by white arrows) of wild-type and morphant larvae contain hair cells of indistinguishable numbers and morphology.

Abbreviations are as follows: cr, crista (sensory patch of inner ear); ep, epithelial protrusions; o, otolith; and pc, posterior semicircular canal.

a structural role during morphogenetic processes, consistent with its expression in the tips of the epithelial projections of the forming semicircular canals and with the described role of other GAGs such as hyaluronic acid during zebrafish inner-ear morphogenesis.[34] In addition, as a component of proteoglycans-like aggrecan or versican, CS might feed back to BMP or other growth-factor signaling, consistent with the described activities of proteoglycans as growth-factor binding proteins and/or coreceptors.[35] For instance, an undulated notochord phenotype as in zebrafish *chsy1* morphants is also displayed by *wnt5a* mutants,[36] pointing to a possible involvement of CHSY1 in noncanonical WNT signaling. Furthermore, as described in detail in the accompanying work by Tian et al.,[37] CHSY1 could modulate signaling through the Notch receptor. CHSY1 has a Fringe domain, which is possibly involved in glycosylation of Notch receptors and thus modifying their ligand specificity and signaling efficiency.[38] Consistent with a role of Chsy1 in reducing Notch signaling, we found that conditional expression of the constitutively active intracellular domain of Notch in zebrafish causes compromised semicircular-canal formation, as does loss of Chsy1 activity (K.L. and M.H., unpublished data). Together, the negative role of Bmp signaling on *chsy1* expression and the negative role of Chsy1 on Notch signaling are in line with the synergistic effect of Notch function downstream of Bmp signaling as reported in many different developmental and physiological scenarios.[39]

In conclusion, we show that loss of human CHSY1 function causes autosomal-recessive Temtamy preaxial brachydactyly syndrome and that antisense-mediated *chsy1* knockdown in zebrafish causes similar defects in multiple developmental processes. In the inner ears of zebrafish larvae, unrestricted Bmp2b signaling or loss of Dan activity leads to reduced *chsy1* expression and, during epithelial morphogenesis, defects similar to those that occur upon Chsy1 inactivation, indicating that Bmp signaling affects inner-ear development by suppressing Chsy1.

## Supplemental Data

Supplemental Data include three figures and two tables and are available with this article online at http://www.cell.com/AJHG/.

## Acknowledgments

We are thankful to all family members who participated in this study, Esther Milz and Evelin Fahle for excellent technical assistance, and Karin Boss for critical reading of the manuscript. This work was supported by the German Federal Ministry of Education and Research (BMBF) by grant number 01GM0880 (SKELNET) and by 01GM0801 (E-RARE network CRANIRARE) to B.W. Work in M.H.'s laboratory was supported by the National Institutes of Health (grant 1R01 GM63904) and the German Research Foundation (SFB572).

Received: August 7, 2010
Revised: October 3, 2010
Accepted: October 7, 2010
Published online: December 2, 2010

## Web Resources

The URLs for data presented herein are as follows:
ENSEMBL, http://www.ensembl.org
UCSC Genome Browser, http://www.genome.ucsc.edu
Online Mendelian Inheritance in Man (OMIM), http://www.ncbi.nlm.nih.gov/omim
PolyPhen, http://coot.embl.de/PolyPhen

## Accession Numbers

CHSY1: MIM 608183. Temtamy preaxial brachydactyly syndrome: OMIM, MIM 605282.

## References

1. Mundlos, S. (2009). The brachydactylies: A molecular disease family. Clin. Genet. *76*, 123–136.
2. Gong, Y., Krakow, D., Marcelino, J., Wilkin, D., Chitayat, D., Babul-Hirji, R., Hudgins, L., Cremers, C.W., Cremers, F.P., Brunner, H.G., et al. (1999). Heterozygous mutations in the gene encoding noggin affect human joint morphogenesis. Nat. Genet. *21*, 302–304.
3. Dawson, K., Seeman, P., Sebald, E., King, L., Edwards, M., Williams, J., 3rd, Mundlos, S., and Krakow, D. (2006). GDF5 is a second locus for multiple-synostosis syndrome. Am. J. Hum. Genet. *78*, 708–712.
4. Temtamy, S.A., Meguid, N.A., Ismail, S.I., and Ramzy, M.I. (1998). A new multiple congenital anomaly, mental retardation syndrome with preaxial brachydactyly, hyperphalangism, deafness and orodental anomalies. Clin. Dysmorphol. *7*, 249–255.
5. Lieschke, G.J., and Currie, P.D. (2007). Animal models of human disease: Zebrafish swim into view. Nat. Rev. Genet. *8*, 353–367.
6. Race, H., Hall, C.M., Harrison, M.G., Quarrell, O.W., and Wakeling, E.L. (2010). A distinct autosomal recessive disorder of limb development with preaxial brachydactyly, phalangeal duplication, symphalangism and hyperphalangism. Clin. Dysmorphol. *19*, 23–27.
7. Abecasis, G.R., Cherny, S.S., Cookson, W.O., and Cardon, L.R. (2001). GRR: Graphical representation of relationship errors. Bioinformatics *17*, 742–743.
8. O'Connell, J.R., and Weeks, D.E. (1998). PedCheck: A program for identification of genotype incompatibilities in linkage analysis. Am. J. Hum. Genet. *63*, 259–266.
9. Abecasis, G.R., Cherny, S.S., Cookson, W.O., and Cardon, L.R. (2002). Merlin—Rapid analysis of dense genetic maps using sparse gene flow trees. Nat. Genet. *30*, 97–101.
10. Kruglyak, L., Daly, M.J., Reeve-Daly, M.P., and Lander, E.S. (1996). Parametric and nonparametric linkage analysis: A unified multipoint approach. Am. J. Hum. Genet. *58*, 1347–1363.
11. Strauch, K., Fimmers, R., Kurz, T., Deichmann, K.A., Wienker, T.F., and Baur, M.P. (2000). Parametric and nonparametric multipoint linkage analysis with imprinting and two-locus-trait models: application to mite sensitization. Am. J. Hum. Genet. *66*, 1945–1957.
12. Thiele, H., and Nürnberg, P. (2005). HaploPainter: A tool for drawing pedigrees with complex haplotypes. Bioinformatics *21*, 1730–1732.
13. Rüschendorf, F., and Nürnberg, P. (2005). ALOHOMORA: A tool for linkage analysis using 10K SNP array data. Bioinformatics *21*, 2123–2125.
14. Hammerschmidt, M., Pelegri, F., Mullins, M.C., Kane, D.A., van Eeden, F.J., Granato, M., Brand, M., Furutani-Seiki, M., Haffter, P., Heisenberg, C.P., et al. (1996). dino and mercedes, two genes regulating dorsal development in the zebrafish embryo. Development *123*, 95–102.
15. Herzog, W., Zeng, X., Lele, Z., Sonntag, C., Ting, J.W., Chang, C.Y., and Hammerschmidt, M. (2003). Adenohypophysis formation in the zebrafish and its dependence on sonic hedgehog. Dev. Biol. *254*, 36–49.
16. Zhang, J., Lefebvre, J.L., Zhao, S., and Granato, M. (2004). Zebrafish unplugged reveals a role for muscle-specific kinase homologs in axonal pathway choice. Nat. Neurosci. *7*, 1303–1309.
17. Mowbray, C., Hammerschmidt, M., and Whitfield, T.T. (2001). Expression of BMP signalling pathway members in the developing zebrafish inner ear and lateral line. Mech. Dev. *108*, 179–184.
18. Whitfield, T.T., Granato, M., van Eeden, F.J., Schach, U., Brand, M., Furutani-Seiki, M., Haffter, P., Hammerschmidt, M., Heisenberg, C.P., Jiang, Y.J., et al. (1996). Mutations affecting development of the zebrafish inner ear and lateral line. Development *123*, 241–254.
19. Yan, Y.-L., Miller, C.T., Nissen, R.M., Singer, A., Liu, D., Kirn, A., Draper, B., Willoughby, J., Morcos, P.A., Amsterdam, A., et al. (2002). A zebrafish sox9 gene required for cartilage morphogenesis. Development *129*, 5065–5079.
20. Peal, D.S., Burns, C.G., Macrae, C.A., and Milan, D. (2009). Chondroitin sulfate expression is required for cardiac atrioventricular canal formation. Dev. Dyn. *238*, 3103–3110.
21. Nasevicius, A., and Ekker, S.C. (2000). Effective targeted gene 'knockdown' in zebrafish. Nat. Genet. *26*, 216–220.
22. Robu, M.E., Larson, J.D., Nasevicius, A., Beiraghi, S., Brenner, C., Farber, S.A., and Ekker, S.C. (2007). p53 activation by knockdown technologies. PLoS Genet. *3*, e78.
23. Rupp, R.A., Snider, L., and Weintraub, H. (1994). Xenopus embryos regulate the nuclear localization of XMyoD. Genes Dev. *8*, 1311–1323.
24. Petko, J.A., Kabbani, N., Frey, C., Woll, M., Hickey, K., Craig, M., Canfield, V.A., and Levenson, R. (2009). Proteomic and functional analysis of NCS-1 binding proteins reveals novel

signaling pathways required for inner ear development in zebrafish. BMC Neurosci. *10*, 27.
25. Chocron, S., Verhoeven, M.C., Rentzsch, F., Hammerschmidt, M., and Bakkers, J. (2007). Zebrafish Bmp4 regulates left-right asymmetry at two distinct developmental time points. Dev. Biol. *305*, 577–588.
26. Whitfield, T.T., Riley, B.B., Chiang, M.-Y., and Phillips, B. (2002). Development of the zebrafish inner ear. Dev. Dyn. *223*, 427–458.
27. Hammond, K.L., Loynes, H.E., Mowbray, C., Runke, G., Hammerschmidt, M., Mullins, M.C., Hildreth, V., Chaudhry, B., and Whitfield, T.T. (2009). A late role for bmp2b in the morphogenesis of semicircular canal ducts in the zebrafish inner ear. PLoS ONE *4*, e4368.
28. Omata, Y., Nojima, Y., Nakayama, S., Okamoto, H., Nakamura, H., and Funahashi, J. (2007). Role of Bone morphogenetic protein 4 in zebrafish semicircular canal development. Dev. Growth Differ. *49*, 711–719.
29. Kitagawa, H., Uyama, T., and Sugahara, K. (2001). Molecular cloning and expression of a human chondroitin synthase. J. Biol. Chem. *276*, 38721–38726.
30. Sugahara, K., Mikami, T., Uyama, T., Mizuguchi, S., Nomura, K., and Kitagawa, H. (2003). Recent advances in the structural biology of chondroitin sulfate and dermatan sulfate. Curr. Opin. Struct. Biol. *13*, 612–620.
31. Bok, J., Brunet, L.J., Howard, O., Burton, Q., and Wu, D.K. (2007). Role of hindbrain in inner ear morphogenesis: Analysis of Noggin knockout mice. Dev. Biol. *311*, 69–78.
32. Nie, X., Luukko, K., and Kettunen, P. (2006). BMP signalling in craniofacial development. Int. J. Dev. Biol. *50*, 511–521.
33. Chang, W., Lin, Z., Kulessa, H., Hebert, J., Hogan, B.L., and Wu, D.K. (2008). Bmp4 is essential for the formation of the vestibular apparatus that detects angular head movements. PLoS Genet. *4*, e1000050.
34. Busch-Nentwich, E., Söllner, C., Roehl, H., and Nicolson, T. (2004). The deafness gene dfna5 is crucial for ugdh expression and HA production in the developing ear in zebrafish. Development *131*, 943–951.
35. Domowicz, M.S., Cortes, M., Henry, J.G., and Schwartz, N.B. (2009). Aggrecan modulation of growth plate morphogenesis. Dev. Biol. *329*, 242–257.
36. Rauch, G.-J., Hammerschmidt, M., Blader, P., Schauerte, H.E., Strähle, U., Ingham, P.W., McMahon, A.P., and Haffter, P. (1997). Wnt5 is required for tail formation in the zebrafish embryo. Cold Spring Harb. Symp. Quant. Biol. *62*, 227–234.
37. Tian, J., Ling, L., Shboul, M., Lee, H., O'Connor, B., Merriman, B., Nelson, F., Cool, S., Ababneh, O.H., Al-Hadidy, A., et al. (2010). Loss of CHSY1, a secreted FRINGE enzyme, causes syndromic brachydactyly and increased NOTCH signaling in humans. Am. J. Hum. Genet. *87*, this issue, 768–778.
38. Yin, L. (2005). Chondroitin synthase 1 is a key molecule in myeloma cell-osteoclast interactions. J. Biol. Chem. *280*, 15666–15672.
39. Guo, X., and Wang, X.F. (2009). Signaling cross-talk between TGF-beta/BMP and other pathways. Cell Res. *19*, 71–88.
40. Piotrowski, T., and Nüsslein-Volhard, C. (2000). The endoderm plays an important role in patterning the segmented pharyngeal region in zebrafish (Danio rerio). Dev. Biol. *225*, 339–356.
41. Stemple, D.L., Solnica-Krezel, L., Zwartkruis, F., Neuhauss, S.C., Schier, A.F., Malicki, J., Stainier, D.Y., Abdelilah, S., Rangini, Z., Mountcastle-Shah, E., and Driever, W. (1996). Mutations affecting development of the notochord in zebrafish. Development *123*, 117–128.